Published in final edited form as:
*Arthritis Rheum*. 2012 August ; 64(8): 2579–2588. doi:10.1002/art.34463.

# Interruption of Glycosphingolipid Synthesis Enhances Osteoarthritis Development in Mice

**Naoki Seito**[1], **Tadashi Yamashita**[2,3], **Yukinori Tsukuda**[1], **Yuichiro Matsui**[1], **Atsushi Urita**[1], **Tomohiro Onodera**[1], **Takeomi Mizutani**[4], **Hisashi Haga**[4], **Naoki Fujitani**[5], **Yasuro Shinohara**[5], **Akio Minami**[1], and **Norimasa Iwasaki**[1]

[1]Department of Orthopaedic Surgery, Hokkaido University Graduate School of Medicine, Sapporo, Japan.

[2]Graduate School of Advanced Life Science, Hokkaido University, Sapporo, Japan.

[3]World Class University Program, Kyungpook National University School of Medicine, Daegu, South Korea.

[4]Transdisciplinary Life Science Course, Faculty of Advanced Life Science, Hokkaido University, Sapporo, Japan.

[5]Laboratory of Medical and Functional Glycomics, Graduate School of Advanced Life Science, Hokkaido University, Sapporo, Japan.

## Abstract

**Objective—**Glycosphingolipids (GSLs) are ubiquitous membrane components that modulate transmembrane signaling and mediate cell-to-cell and cell-to-matrix interactions. GSL expression is decreased in the articular cartilage of humans with osteoarthritis (OA). The aim of this study was to determine the functional role of GSLs in cartilage metabolism related to OA pathogenesis.

**Methods—**We generated mice with knockout of the chondrocyte-specific *Ugcg*, which encodes an initial enzyme of major GSL synthesis, (Col2-*Ugcg*$^{-/-}$), using the Cre/loxP system. *In vivo* OA and *in vitro* cartilage degradation models were used to evaluate the effect of GSLs on cartilage degradation process.

**Results—**Although Col2-*Ugcg*$^{-/-}$ mice developed and grew normally, osteoarthritic changes were dramatically enhanced with aging through the overexpression of MMP-13 and chondrocyte apoptosis compared to their wild-type (WT) littermates. Col2-*Ugcg*$^{-/-}$ mice showed more severe instability-induced pathologic OA *in vivo* and interleukin-1α (IL-1α) induced cartilage degradation *in vitro*. IL-1α stimulation of chondrocytes from WT mice significantly increased *Ugcg* mRNA expression and upregulated GSL metabolism.

**Conclusion—**GSL deficiency in chondrocytes enhances the development of OA. On the other hand, the deficiency does not affect the development and organization of cartilage tissue at a young age. These findings indicate that GSLs maintain cartilage molecular metabolism and prevent disease progression, although GSLs are not essential for chondrogenesis of progenitor and stem cells and cartilage development in young mice. GSL metabolism in the cartilage is a potential target for developing a novel treatment for OA.

Address correspondence to: Norimasa Iwasaki, MD, PhD, Department of Orthopaedic Surgery, Hokkaido University Graduate School of Medicine. Kita 15, Nishi 7, Kita-ku, Sapporo 060-8638, Japan. Phone: 81-11-706-5937, Fax: 81-11-706-6054. niwasaki@med.hokudai.ac.jp. To whom correspondence may be addressed. Tadashi Yamashita, DVM, PhD, ty11106@sci.hokudai.ac.jp.

Osteoarthritis (OA), the most common joint disease, affects over 200 million people worldwide (1, 2) and frequently leads to disabilities in performing daily activities among the elderly. The disease costs the United States economy more than $60 billion per year (3). OA is characterized by degradation of the cartilage extracellular matrix. Elucidation of the pathogenesis of OA requires a better understanding of the cartilage degradation mechanism. Despite the large number of gene-based or protein-based studies performed to clarify the mechanism of cartilage degradation, the pathogenesis of this joint disease remains unclear. A new molecular target is therefore needed to analyze the mechanism of cartilage degradation.

Glycosphingolipids (GSLs) are ubiquitous membrane components. They are a diverse group of complex lipids that contain the hydrophobic ceramide moiety and a hydrophilic oligosaccharide residue. Their lipid portion, ceramide, is embedded in the outer leaflet of the plasma membrane, and their oligosaccharide moieties project into the extracellular space (4, 5). GSLs form clusters on cell membranes and modulate transmembrane signaling and mediate cell-to-cell and cell-to-matrix interactions (4–9). The first committed step in the synthesis of the majority of GSLs is directed by the enzyme glucosylceramide synthase, encoded by the *Ugcg* gene (Figure 1 A) (4, 10–12). The enzyme catalyzes the transfer of a glucose moiety from UDP-glucose to ceramide to form glucosylceramide, the precursor to most cellular GSLs with hundreds of different oligosaccharide structures. Mice with a global disruption in *Ugcg* are embryonic lethal (E7.5), suggesting that GSLs are essential for embryonic development and differentiation (11, 12).

To date, the tissue specific functions of GSLs in the nervous system and epidermis have been concretely clarified using conditional knockout (KO) mice (10, 13, 14). Regarding articular cartilage, GSL expression of chondrocytes is decreased in human OA samples (15, 16). Chondrocytes are the only cells in cartilage responsible for the synthesis and degradation of the extracellular matrix. Decreased GSL expression leads to alterations in the biochemical composition of the chondrocyte membrane (15). The role of these changes in cartilage metabolism and in the pathogenesis of OA, however, is unknown.

Here, we hypothesized that alterations of chondrocyte GSLs could be responsible for disturbances in cartilage homeostasis, contributing to the development of OA. To test this hypothesis, we generated KO mice of the chondrocyte-specific *Ugcg* for GSL deficiency in chondrocytes. The current study demonstrated that chondrocyte-specific GSL deficiency accelerated the development of OA under physiological and pathological conditions through enhancement of chondrocyte MMP-13 secretion and apoptosis. These findings indicate that GSLs are key molecules contributing to the pathogenesis of OA.

## MATERIALS AND METHODS

### Generation of chondrocyte-specific *Ugcg* KO mice

To interrupt GSL synthesis in cartilage, we generated mice with knockout of the chondrocyte-specific *Ugcg* (Col2-*Ugcg*$^{-/-}$) by crossing *Ugcg*$^{loxP/loxP}$ mice (10) with Col2a1-Cre transgenic mice (17), in which Cre recombinase is expressed specifically in chondrocytes under the Col2a1 promoter. Transgenic mice carrying the Col2a1-Cre transgene (Strain Name: B6; SJL-Tg [Col2a1-Cre] 1Bhr/J; Stock Number: 003554) were obtained from The Jackson Laboratory (Bar Harbor, ME). *Ugcg*$^{loxP/loxP}$ mice were generated on a C57BL/6 background as previously described (17). Col2-*Ugcg*$^{-/-}$ mice were generated by breeding Col2a1-Cre transgenic mice with *Ugcg*$^{loxP/loxP}$ mice. Wild-type littermates (*Ugcg*$^{loxP/loxP}$) were used as controls. Genotyping was accomplished by PCR of tail DNA using primer sets as previously described (10). Mice were housed in a temperature- and humidity-controlled environment on a 12-h light-dark cycle and fed a

standard rodent diet. All experiments were performed according to the protocol approved by the Institute of Animal Care and Use Committee of the Hokkaido University Graduate School of Medicine.

### Skeletal staining

To observe the skeletal systems, whole skeletons of wild-type (WT) and Col2-*Ugcg*$^{-/-}$ littermates were stained with alcian blue and alizarin red as previously described (18, 19).

### Age-associated OA model

At 4, 12, and 15 months of age, mice were euthanized and their entire knee joints were dissected to assess the spontaneous development of OA, as an age-associated OA model (20, 21).

### Instability-induced OA model

An OA model was created in 8-week-old mice by destabilizing the knee joint as previously described (20, 22). Under general anesthesia, the right knee joint was destabilized by transection of the medial collateral ligament and removal of the cranial half of the medial meniscus using a microsurgical technique (OA side). A sham operation was performed on the left knee joint using the same approach without ligament transection and meniscectomy (sham side). To assess the histological findings, the mice were euthanized and entire knee joints were dissected 8 weeks after surgery.

### Histological analysis

For hematoxylin and eosin (HE) and safranin-O staining, samples were fixed in 10% buffered formalin and decalcified in 10% EDTA (pH 7.5). Each tissue was dehydrated and embedded in paraffin, and sectioned into 5-μm thick slices. Chondrocyte number and cartilage thickness were quantified as previously described (20, 23–25). Three observers who were blinded to the experimental group quantified the OA severity using the Mankin scoring system (26, 27) and those scores were averaged.

### Immunohistochemistry

Sections of the knee were deparaffinized and quenched for endogenous peroxidase activity. After treatment with chondroitinase ABC (0.25 U/ml), the sections were incubated with polyclonal antibody (1:200 dilution) against the carboxyl terminus of MMP-13 (Chemicon, Temecula, CA) and monoclonal antibody (1:10 dilution) against ceramide (Alexis, San Diego, CA) at 4°C overnight. After washing with phosphate-buffered saline 3 times, the samples were incubated with a biotinylated secondary antibody. Type II and X collagens were identified using polyclonal rabbit antibodies against rat type II and X collagens (LSL, Tokyo, Japan).

### Terminal deoxynucleotidyl transferase dUTP nick-end labeling (TUNEL) assay

To investigate chondrocyte apoptosis, the TUNEL assay was performed using an *in situ* Apoptosis Detection Kit (Takara Shuzo, Kyoto, Japan) according to the manufacturer's instructions.

### Proteoglycan release from cultured cartilage explants

*In vitro* cartilage catabolism was analyzed by culturing mouse femoral head cartilage with IL-1α (Sigma, St. Louis, MO) (20, 28). The femoral head cartilage was harvested from 4-week-old mice and pre-cultured for 48 hours at 37°C in a humidified atmosphere of 5% CO2 and 95% air in Dulbecco's modified Eagle's medium (DMEM) containing 1% antibiotic

solution, 2 mM glutamine, 10 mM HEPES, 50 μg/ml ascorbate, and 10% fetal bovine serum. The explants were then washed 3 times and cultured for an additional 72 hours in serum-free DMEM plus 10 ng/ml mouse IL-1α. To quantify the proteoglycan release from cartilage explants with cartilage degradation, the proteoglycan content in the medium and digested cartilage was measured as sulfated glycosaminoglycan using a dimethylmethylene blue assay as previously described (20, 28). The amount of proteoglycan released from a cartilage explant into the medium was quantitatively expressed as the percentage release of proteoglycan (%RPG, proteoglycan amount in the medium / total amount of proteoglycan in the serum and cartilage explants × 100).

### Isolation of chondrocytes

Immature mouse chondrocytes were obtained from the hip and knee joints of 6-day-old mice as previously described (29, 30). Briefly, cartilage specimens were treated with 0.25% trypsin (Wako Pure Chemical Industries, Osaka, Japan) in sterile saline for 30 minutes followed by 0.25% collagenase (Gibco/Invitrogen, Grand Island, NY) in DMEM containing 1% antibiotic solution and 10% fetal bovine serum for 4 hours at 37°C in a culture bottle. Isolated primary chondrocytes were cultured for 24 hours in serum-free DMEM plus 10 ng/ml mouse IL-1α for further analysis.

### Enzyme-linked immunosorbent assay (ELISA)

MMP-13 in the chondrocyte culture supernatant was measured using an ELISA kit for mouse MMP-13 (Uscnlife, Missouri, TX) according to the manufacturer's instructions.

### Quantification of nitric oxide

Nitric oxide was quantified based on the amount of its stable end product, nitrite, in the chondrocyte culture supernatant (31). Griess Reagent System (Promega, Madison, WI) was used for this assay according to the manufacturer's instructions.

### Cellular stiffness measurement

As mentioned above, GSLs exist on cell membranes. Therefore, we hypothesized that loss of GSLs would lead to alterations in the mechanical properties of the chondrocyte membrane. To test this hypothesis, we directly visualized a single chondrocyte and quantitatively measured the cellular stiffness using an atomic force microscope as previously described (32). A customized atomic force microscope system (33) and a commercial cantilever (MLCT-AUNM; Veeco Instruments, Santa Barbara, CA) with a spring constant of 0.01 N/m were chosen for the measurement. The details of the stiffness measurement were described previously (34, 35).

### Quantitative real-time reverse transcriptase-polymerase chain reaction (RT-PCR)

Total RNA was extracted from the samples using a Qiagen RNeasy MINI Kit (Qiagen, Valencia, CA). For cDNA synthesis, 0.5 or 1.0 μg of RNA was reverse-transcribed using random hexamer primers (Promega, Madison, WI) and Improm-II reverse transcriptase (Promega). Real-time RT-PCR was performed using an OPTICON II (Bio-Rad Laboratories, Hercules, CA). Signals were detected using a SYBR Green qPCR Kit (Finzymes, Espoo, Finland) with the following gene-specific primers: *Ugcg*, 5'-AGC TGG AGA ACT GGT CGC TA-3' (forward) and 5'-CAC ACT GTG CGC CAT CAG-3' (reverse); MMP-13, 5'-TTGGCCACTCCCTAGGTCTG-3' (forward) and 5'-GGTTGGGGTCTTCATCGC-3' (reverse); iNOS, 5'-ACATCGACCCGTCCACAGTAT-3' (forward) and 5'-CAGAGGGGTAGGCTTGTCTC-3' (reverse); and glyceraldehyde 3-phosphate dehydrogenase (GAPDH), 5'-ACTTTGTCAAGCTCATTTCC-3' (forward) and 5'-TGCAGCGAACTTTATTGATG-3' (reverse) as a control housekeeping gene. The

relative mRNA expression of each targeted gene was expressed by the cycle threshold (Ct) value of each gene normalized to the Ct value of GAPDH.

### Quantification of GSLs in the cultured chondrocytes

GSLs were extracted from mouse chondrocyte pellets. To quantify the GSLs content, glycans of GSLs were digested by enzymatic reaction employing GSL-specific endoglycoceramidases II (EGCase II) derived from mutant strain M-750 of *Rhodococcus* sp. (Takara Bio, Otsu, Japan). The solutions treated by EGCase were subjected to glycoblotting using a protocol similar to that used for *N*-glycome analyses reported previously (36, 37). Samples were applied to Matrix Assisted Laser Desorption Ionization - Time of Flight mass spectrometry (MALDI-TOF MS) analysis on an Ultraflex II TOF/TOF mass spectrometer (Bruker Daltonics GmbsH, Bremen, Germany) equipped with a reflector, and controlled by the FlexControl 3.0 software package (Bruker Daltonics). Peaks were detected as proton-adducted ions. Masses were annotated using the FlexAnalysis 3.0 software package (Bruker Daltonics). In addition to TOF/TOF analyses, we used the database GlycoSuiteDB (http://glycosuitedb.expasy.org/glycosuite/glycodb) and SphinGOMAP© (http://www.sphingomap.org/) for the structural identification of glycans.

### Statistical analysis

Data are expressed as mean ± standard error of the mean (SEM). Means of groups were compared by two-tailed unpaired *t*-tests. *P* values less than 0.05 were considered significant.

## RESULTS

### Confirmation of chondrocyte-specific *Ugcg* deletion

The tissue specificity of recombination was confirmed by PCR of genomic DNA using primer sets (10) that detected either the intact $Ugcg^{loxP}$ allele (primers 1 and 2) or the Cre-recombined $Ugcg^{\Delta}$ allele (primers 1 and 3) (Figures 1B and C). We next used real-time RT-PCR to determine the relative *Ugcg* mRNA levels in the cartilage of Col2-$Ugcg^{-/-}$ mice and WT littermates ($Ugcg^{loxP/loxP}$) (Figure 1D). Real-time RT-PCR analysis showed that *Ugcg* mRNA expression was reduced by greater than 80% in the articular cartilage of Col2-$Ugcg^{-/-}$ mice, compared to that in WT littermates (n = 3 per each group, $P < 0.05$). Furthermore, we confirmed *Ugcg* mRNA deletion in the cartilage, but not in other tissues including the brain, liver, kidney, and spleen (data not shown).

### Col2-$Ugcg^{-/-}$ mice developed and grew normally in young age

Col2-$Ugcg^{-/-}$ mice developed and grew normally without abnormalities of major organs and could not be distinguished from WT littermates. The whole skeletons of newborn mice stained with alcian blue and alizarin red did not differ in appearance between genotypes (Figure 2A). Body weight did not differ significantly between genotypes in growth curves (Figure 2B). Histological examination of the knee joints in 4-week-old mice showed that chondrocyte number, cartilage thickness, and growth plate width of Col2-$Ugcg^{-/-}$ mice were similar to those of WT littermates (Figure 2C, Supplemental Figure S1A). Safranin-O staining and immunostaining of type II and X collagen were comparable between WT and Col2-$Ugcg^{-/-}$ littermates (Figure 2C). The expression levels of the MMP-13, ADAMTS4, and ADATTS5 mRNA were also comparable between genotypes (Supplemental Figure S1B). The glycosaminoglycan composition in the cartilage of Col2-$Ugcg^{-/-}$ mice was similar to that of WT littermates (Supplemental Table 1). To assess the mechanical properties of chondrocytes, we directly visualized a single chondrocyte and quantitatively measured the stiffness of the cell using an atomic force microscope. There was no significant difference in the value between the two genotypes (Supplemental Figure S2A).

Furthermore, proliferation and matrix production of chondrocytes were not significantly different between the two genotypes *in vitro* (Supplemental Figure S2B).

## Chondrocyte-specific deletion of GSLs enhances the development of OA with aging by inducing overexpression of MMP-13 and chondrocyte apoptosis

Mice were followed up to 15 months of age to assess the spontaneous development of OA with aging. There were no apparent osteoarthritic changes in the knee joints in either genotype at 4 months of age (Figure 3A). At 12 and 15 months of age, slight, but significant, osteoarthritic changes were detected in the knee joints of WT mice. There were mild, superficial cartilage erosion, and slight reduction of safranin-O staining at each time point (Figure 3A). On the other hand, these osteoarthritic changes were more progressed in Col2-*Ugcg*$^{-/-}$ mice at 12 and 15 months of age, compared to those of WT littermates (data at 12 months of age not shown) (Figure 3A). These histological findings were quantitatively confirmed using the Mankin grading score (n = 10 per each group at each time, 3.65 ± 0.39 in WT mice vs. 5.77 ± 0.40 in Col2-*Ugcg*$^{-/-}$ mice at 12 months, $P < 0.01$; 4.95 ± 0.30 in WT mice vs. 6.87 ± 0.38 in Col2-*Ugcg*$^{-/-}$ mice at 15 months, $P < 0.01$) (Figure 3B). Next, we performed the immunostaining of MMP-13 (Figure 3A) and quantified the percentage of MMP-13 positive cells (Figure 3C). Although no significant difference in MMP-13 expression was found between either genotype at 4 months of age, MMP-13 expression increased at a greater rate in Col2-*Ugcg*$^{-/-}$ mice with aging, compared to WT littermates (n = 10 per each group at each time, 11.37 ± 0.56% in WT mice vs. 17.22 ± 0.90% in Col2-*Ugcg*$^{-/-}$ mice at 12 months, $P < 0.01$; 12.18 ± 0.65% in WT mice vs. 21.07 ± 1.08% in Col2-*Ugcg*$^{-/-}$ mice at 15 months, $P < 0.01$). Furthermore, TUNEL positive cells significantly increased in Col2-*Ugcg*$^{-/-}$ mice with aging, compared to WT littermates (n = 10 per each group at each time, 3.86 ± 0.25% in WT mice vs. 7.58 ± 0.44% in Col2-*Ugcg*$^{-/-}$ mice at 12 months, $P < 0.01$; 10.07 ± 0.46% in WT mice vs. 21.48 ± 1.75% in Col2-*Ugcg*$^{-/-}$ mice at 15 months, $P < 0.01$) (Figure 3A and D). In addition, we confirmed whether or not interruption of *Ugcg* gene expression increased the ceramide content in chondrocytes. Immunostaining of ceramide by the anti-ceramide antibody produced a similar staining pattern between the 2 genotypes at each time point (Supplemental Figure S3A). No significant difference in the percentage of ceramide positive cells was found at any time point (Supplemental Figure S3B).

## Chondrocyte-specific deletion of GSLs enhances the development of instability-induced OA

We analyzed the development of instability-induced OA changes in WT and Col2-*Ugcg*$^{-/-}$ littermates. Sham operations for both genotypes produced no significant osteoarthritic changes. In the joints of WT mice at 8 weeks after instability-induced surgery, osteoarthritic changes developed such as cartilage erosion and reduction of safranin-O staining and chondrocyte number (Figure 4A). The deletion of GSLs showed more severe osteoarthritic changes. In the joints of Col2-*Ugcg*$^{-/-}$ mice at 8 weeks after surgery, the uncalcified zone (upper layer above the tidemark) was almost completely lost and the number of chondrocytes was significantly reduced (Figure 4A). The quantitative assessment using the Mankin grading score supported these histological findings (n = 8 per group, 5.70 ± 0.55 in WT mice vs. 10.96 ± 0.46 in Col2-*Ugcg*$^{-/-}$ mice, $P < 0.01$) (Figure 4B).

## Chondrocyte-specific deletion of GSLs enhances cartilage degradation by IL-1α stimulation

To understand the mechanism of the decreased proteoglycan levels in OA joints, we performed *in vitro* experiments. Cartilage explants were maintained in culture with IL-1α, and the release of proteoglycan into the medium determined by using a dimethylmethylene blue assay. Under the *in vitro* conditions, Col2-*Ugcg*$^{-/-}$ cartilage increased %RPG more

significantly than did WT cartilage by IL-1α stimulation (n = 5 per group, 37.66 ± 0.88 % in WT mice vs. 53.05 ± 0.81 % in Col2-*Ugcg*$^{-/-}$ mice, $P < 0.01$) (Figure 5A). Histological examination of the explants also demonstrated that safranin-O staining for proteoglycans was reduced more in Col2-*Ugcg*$^{-/-}$ cartilage than in WT cartilage (Figure 5B). Furthermore, immunostaining of MMP-13 strongly enhanced in Col2-*Ugcg*$^{-/-}$ cartilage, compared to WT cartilage (Figure 5B). And we found the significant elevation of both MMP-13 mRNA (n = 5 per group, 6.75 ± 0.73 in WT vs. 11.00 ± 1.41 in Col2-*Ugcg*$^{-/-}$, $P < 0.05$) and protein expression (n = 5 per group, 238.18 ± 7.09 pg/ml in WT vs. 307.58 ± 9.97 pg/ml in Col2-*Ugcg*$^{-/-}$, $P < 0.05$) in Col2-*Ugcg*$^{-/-}$ chondrocytes, compared to those of WT chondrocytes (Figure 6A and B). TUNEL staining also enhanced in Col2-*Ugcg*$^{-/-}$ cartilage, compared to WT cartilage (Figure 5B). And we found the significant elevation of both inducible nitric oxide synthase (iNOS) mRNA expression (n = 5 per group, 1.10 ± 0.10 in WT vs. 2.00 ± 0.24 in Col2-*Ugcg*$^{-/-}$, $P < 0.05$) and nitric oxide production (n = 5 per group, 52.16 ± 0.16 μM in WT vs. 60.30 ± 0.13 μM in Col2-*Ugcg*$^{-/-}$, $P < 0.05$) in Col2-*Ugcg*$^{-/-}$ chondrocytes, compared to those of WT chondrocytes (Figure 6C and D).

### IL-1α can increase *Ugcg* mRNA level and upregulate the GSL metabolism in WT chondrocytes

Isolated primary chondrocytes from WT mice were cultured for 24 hours in serum-free DMEM with or without IL-1α for further analysis. Real-time RT-PCR analysis showed that IL-1α stimulation significantly increased *Ugcg* mRNA expression from $4.89 \times 10^{-2} \pm 0.43 \times 10^{-2}$ to $9.02 \times 10^{-2} \pm 1.48 \times 10^{-2}$ in WT chondrocytes (n = 5, $P < 0.05$) (Figure 6E). Next, to quantify the total amount of GSLs in cultured chondrocytes, we extracted GSLs from cultured chondrocyte pellets and measured the amount of the glycans of GSLs using mass spectrometry. This analysis showed that IL-1α stimulation significantly increased the total amount of GSLs in WT chondrocytes from 8.1 ± 1.4 pmol/$1\times10^6$ cells to 35.7 ± 3.5 pmol/$1\times10^6$ cells (n = 3, $P < 0.01$) (Figure 6F). Col2-*Ugcg*$^{-/-}$ chondrocytes showed very low expression of *Ugcg* mRNA and low amount of GSLs both after and before IL-1α stimulation (Figure 6E and F).

## DISCUSSION

Our hypothesis was that alterations of chondrocyte GSLs could result in disturbance in cartilage homeostasis, contributing to the development of OA. To determine the functional significance of GSLs in cartilage, we generated Col2-*Ugcg*$^{-/-}$ mice, which interrupts GSL synthesis in chondrocytes. Col2-*Ugcg*$^{-/-}$ newborn mice showed normal whole skeletons. In addition, the mice developed and grew normally without abnormalities of major organs. Histological and immunohistochemical findings of articular cartilage in 4-week old Col2-*Ugcg*$^{-/-}$ mice were comparable to those in WT littermates. No significant differences in proliferation, matrix production, and cellular stiffness of chondrocytes were found between the 2 genotypes. Neural cell-specific deletion of *Ugcg* results in a striking loss of Purkinje cells and abnormal neurologic behavior, suggesting that GSLs are important molecules for neuron differentiation and maturation (10, 14). On the other hand, the current results indicate that chondrocyte-specific deletion of *Ugcg* does not affect the chondrocyte differentiation and the development and organization of cartilage tissue in young mice.

The main purpose of this study was to clarify the functional roles of chondrocyte GSLs in the development of OA. One of the critical causes of OA is considered to be aging. Therefore, we first investigated the roles of GSLs in age-associated OA development. Although there were no apparent osteoarthritic changes in the knee joints in Col2-*Ugcg*$^{-/-}$ mice at 4 months of age, the osteoarthritic findings were more progressed in the mice at 12 and 15 months of age, compared to those of WT littermates. Immunostaining of MMP-13 and TUNEL staining demonstrated a significant increase in MMP-13 expression and

chondrocyte apoptosis of 12 and 15-month-old Col2-*Ugcg*$^{-/-}$ mice. Interruption of *Ugcg* gene expression might increase the ceramide content in chondrocytes (Figure 1A), which induces cellular apoptosis (38, 39). However, the result from immunostaining of ceramide suggests that we can eliminate the direct effects of ceramide accumulation on OA development in Col2-*Ugcg*$^{-/-}$ mice. These results indicate that chondrocyte-specific deletion of GSLs significantly enhances the progression of osteoarthritic changes in articular cartilage associated with aging by inducing overexpression of MMP-13 and chondrocyte apoptosis.

Another critical cause of OA is excessive mechanical stress against joints due to joint instability. Then, we investigated the role of GSLs in OA due to excessive stress against the knee joint by surgically inducing joint instability. Histological findings of instability-induced OA were more progressed in the knees of Col2-*Ugcg*$^{-/-}$ mice compared to those of WT littermates. The obtained findings clearly suggest that the lack of GSLs also results in significant progression of instability-induced OA.

Cartilage degradation in OA is characterized by initial proteoglycan depletion of the cartilage extracellular matrix (34, 40). To elucidate this mechanism, we placed femoral head cartilage in explant culture and stimulated it with IL-1α to promote proteoglycan release. Col2-*Ugcg*$^{-/-}$ cartilage released significantly more total proteoglycan than did WT cartilage. A reduction in safranin O staining of Col2-*Ugcg*$^{-/-}$ cartilage also supported the proteoglycan loss from the explants. These results suggest that chondrocyte-specific deletion of GSLs accelerates cartilage degradation by IL-1α. Furthermore, enhanced immunostaining of MMP-13 and TUNEL staining in Col2-*Ugcg*$^{-/-}$ cartilage strongly suggests that IL-1α stimulation remarkably enhances cartilage degradation through the overexpression of MMP-13 and chondrocyte apoptosis. The significant elevation of both MMP-13 mRNA and protein expression and nitric oxide production in Col2-*Ugcg*$^{-/-}$ chondrocytes after IL-1α stimulation quantitatively confirm these results. The findings obtained from these *in vitro* assessments support the current *in vivo* results in the OA models using conditional KO mice.

This study also demonstrated that IL-1α stimulation significantly increased *Ugcg* mRNA and the total amount of GSLs in WT chondrocytes. A previous study showed that IL-1α stimulation significantly increased hepatic *Ugcg* mRNA level *in vivo* as well as in HepG2 cells *in vitro* as compared to other cytokines (41). Together, these findings suggest that IL-1α can increase chondrocyte *Ugcg* mRNA level, resulting in the upregulation of GSL metabolism, as well as hepatocytes. In contrast, the deletion of this reaction in Col2-*Ugcg*$^{-/-}$ chondrocytes may lead to accelerated cartilage degradation by IL-1α stimulation. The obtained results indicate that loss of GSLs results in greater cartilage vulnerability against IL-1α stimulation in the cartilage degradation process by increasing MMP-13 secretion and apoptosis of chondrocytes. In the next study, we will examine whether GSLs have a chondroprotective function via experiments which overexpress the chondrocyte GSLs. GSLs are present in the plasma membrane of eukaryotic cells, including chondrocytes (42–44). Therefore, we speculate that GSLs participate in modulating signal transduction in the IL-1α pathway related to chondrocyte metabolism. Further studies are required to confirm our speculation.

To our best knowledge, this is the first study to show the functional roles of GSLs in development of OA. Our mechanism-of-action studies suggest that GSLs are potentially regulatory components against chondrocyte MMP-13 secretion and apoptosis, which mainly contribute to the pathogenesis of OA. Currently, there are no pharmacologic treatments that block the development of this disease. Although this mechanism should be further clarified by additional studies, GSLs may become targeting molecules to constitute a novel and effective strategy for the treatment of OA.

## Supplementary Material

Refer to Web version on PubMed Central for supplementary material.

## Acknowledgments

We thank Mr. Mark Hamilton (Tokai University, Sapporo, Japan) for paper preparation.

This work was supported by Health and Labour Sciences Research Grants "Comprehensive Research on Aging and Health" from the Ministry of Health, Labour, and Welfare in Japan and Uehara Memorial Foundation.

## REFERENCES

1. Lin AC, Seeto BL, Bartoszko JM, Khoury MA, Whetstone H, Ho L, et al. Modulating hedgehog signaling can attenuate the severity of osteoarthritis. Nat Med. 2009; 15(12):1421–1425. [PubMed: 19915594]
2. Arai M, Anderson D, Kurdi Y, Annis-Freeman B, Shields K, Collins-Racie LA, et al. Effect of adenovirus-mediated overexpression of bovine ADAMTS-4 and human ADAMTS-5 in primary bovine articular chondrocyte pellet culture system. Osteoarthritis Cartilage. 2004; 12(8):599–613. [PubMed: 15262240]
3. Buckwalter JA, Saltzman C, Brown T. The impact of osteoarthritis: implications for research. Clin Orthop Relat Res. 2004; (427 Suppl):S6–S15. [PubMed: 15480076]
4. Ichikawa S, Hirabayashi Y. Glucosylceramide synthase and glycosphingolipid synthesis. Trends Cell Biol. 1998; 8(5):198–202. [PubMed: 9695839]
5. Varki A. Biological roles of oligosaccharides: all of the theories are correct. Glycobiology. 1993; 3(2):97–130. [PubMed: 8490246]
6. Hakomori S. Bifunctional role of glycosphingolipids. Modulators for transmembrane signaling and mediators for cellular interactions. J Biol Chem. 1990; 265(31):18713–18716. [PubMed: 2229037]
7. Degroote S, Wolthoorn J, van Meer G. The cell biology of glycosphingolipids. Semin Cell Dev Biol. 2004; 15(4):375–387. [PubMed: 15207828]
8. Kolter T, Proia RL, Sandhoff K. Combinatorial ganglioside biosynthesis. J Biol Chem. 2002; 277(29):25859–25862. [PubMed: 12011101]
9. Lingwood D, Simons K. Lipid rafts as a membrane-organizing principle. Science. 327(5961):46–50. [PubMed: 20044567]
10. Yamashita T, Allende ML, Kalkofen DN, Werth N, Sandhoff K, Proia RL. Conditional LoxP-flanked glucosylceramide synthase allele controlling glycosphingolipid synthesis. Genesis. 2005; 43(4):175–180. [PubMed: 16283624]
11. Yamashita T, Wada R, Proia RL. Early developmental expression of the gene encoding glucosylceramide synthase, the enzyme controlling the first committed step of glycosphingolipid synthesis. Biochim Biophys Acta. 2002; 1573(3):236–240. [PubMed: 12417405]
12. Yamashita T, Wada R, Sasaki T, Deng C, Bierfreund U, Sandhoff K, et al. A vital role for glycosphingolipid synthesis during development and differentiation. Proc Natl Acad Sci U S A. 1999; 96(16):9142–9147. [PubMed: 10430909]
13. Jennemann R, Sandhoff R, Langbein L, Kaden S, Rothermel U, Gallala H, et al. Integrity and barrier function of the epidermis critically depend on glucosylceramide synthesis. J Biol Chem. 2007; 282(5):3083–3094. [PubMed: 17145749]
14. Jennemann R, Sandhoff R, Wang S, Kiss E, Gretz N, Zuliani C, et al. Cell-specific deletion of glucosylceramide synthase in brain leads to severe neural defects after birth. Proc Natl Acad Sci U S A. 2005; 102(35):12459–12464. [PubMed: 16109770]
15. David MJ, Hellio MP, Portoukalian J, Richard M, Caton J, Vignon E. Gangliosides from normal and osteoarthritic joints. J Rheumatol Suppl. 1995; 43:133–135. [PubMed: 7752118]
16. David MJ, Portoukalian J, Rebbaa A, Vignon E, Carret JP, Richard M. Characterization of gangliosides from normal and osteoarthritic human articular cartilage. Arthritis Rheum. 1993; 36(7):938–942. [PubMed: 8318040]

17. Ovchinnikov DA, Deng JM, Ogunrinu G, Behringer RR. Col2a1-directed expression of Cre recombinase in differentiating chondrocytes in transgenic mice. Genesis. 2000; 26(2):145–146. [PubMed: 10686612]
18. Yamada T, Kawano H, Koshizuka Y, Fukuda T, Yoshimura K, Kamekura S, et al. Carminerin contributes to chondrocyte calcification during endochondral ossification. Nat Med. 2006; 12(6): 665–670. [PubMed: 16680148]
19. Nakamichi Y, Shukunami C, Yamada T, Aihara K, Kawano H, Sato T, et al. Chondromodulin I is a bone remodeling factor. Mol Cell Biol. 2003; 23(2):636–644. [PubMed: 12509461]
20. Matsui Y, Iwasaki N, Kon S, Takahashi D, Morimoto J, Matsui Y, et al. Accelerated development of aging-associated and instability-induced osteoarthritis in osteopontin-deficient mice. Arthritis Rheum. 2009; 60(8):2362–2371. [PubMed: 19644889]
21. Stoop R, van der Kraan PM, Buma P, Hollander AP, Billinghurst RC, Poole AR, et al. Type II collagen degradation in spontaneous osteoarthritis in C57Bl/6 and BALB/c mice. Arthritis Rheum. 1999; 42(11):2381–2389. [PubMed: 10555034]
22. Clements KM, Price JS, Chambers MG, Visco DM, Poole AR, Mason RM. Gene deletion of either interleukin-1beta, interleukin-1beta-converting enzyme, inducible nitric oxide synthase, or stromelysin 1 accelerates the development of knee osteoarthritis in mice after surgical transection of the medial collateral ligament and partial medial meniscectomy. Arthritis Rheum. 2003; 48(12): 3452–3463. [PubMed: 14673996]
23. Shimizu S, Asou Y, Itoh S, Chung UI, Kawaguchi H, Shinomiya K, et al. Prevention of cartilage destruction with intraarticular osteoclastogenesis inhibitory factor/osteoprotegerin in a murine model of osteoarthritis. Arthritis Rheum. 2007; 56(10):3358–3365. [PubMed: 17907189]
24. Bomsta BD, Bridgewater LC, Seegmiller RE. Premature osteoarthritis in the Disproportionate micromelia (Dmm) mouse. Osteoarthritis Cartilage. 2006; 14(5):477–485. [PubMed: 16431140]
25. Zemmyo M, Meharra EJ, Kuhn K, Creighton-Achermann L, Lotz M. Accelerated, aging-dependent development of osteoarthritis in alpha1 integrin-deficient mice. Arthritis Rheum. 2003; 48(10):2873–2880. [PubMed: 14558093]
26. Mankin HJ. Biochemical and metabolic abnormalities in osteoarthritic human cartilage. Fed Proc. 1973; 32(4):1478–1480. [PubMed: 4121832]
27. Mankin HJ, Dorfman H, Lippiello L, Zarins A. Biochemical and metabolic abnormalities in articular cartilage from osteo-arthritic human hips. II. Correlation of morphology with biochemical and metabolic data. J Bone Joint Surg Am. 1971; 53(3):523–537. [PubMed: 5580011]
28. Glasson SS, Askew R, Sheppard B, Carito B, Blanchet T, Ma HL, et al. Deletion of active ADAMTS5 prevents cartilage degradation in a murine model of osteoarthritis. Nature. 2005; 434(7033):644–648. [PubMed: 15800624]
29. Gosset M, Berenbaum F, Thirion S, Jacques C. Primary culture and phenotyping of murine chondrocytes. Nat Protoc. 2008; 3(8):1253–1260. [PubMed: 18714293]
30. Salvat C, Pigenet A, Humbert L, Berenbaum F, Thirion S. Immature murine articular chondrocytes in primary culture: a new tool for investigating cartilage. Osteoarthritis Cartilage. 2005; 13(3): 243–249. [PubMed: 15727891]
31. Hashimoto S, Takahashi K, Ochs RL, Coutts RD, Amiel D, Lotz M. Nitric oxide production and apoptosis in cells of the meniscus during experimental osteoarthritis. Arthritis Rheum. 1999; 42(10):2123–2131. [PubMed: 10524683]
32. Hsieh CH, Lin YH, Lin S, Tsai-Wu JJ, Herbert Wu CH, Jiang CC. Surface ultrastructure and mechanical property of human chondrocyte revealed by atomic force microscopy. Osteoarthritis Cartilage. 2008; 16(4):480–488. [PubMed: 17869545]
33. Mizutani T, Haga H, Kawabata K. Cellular stiffness response to external deformation: tensional homeostasis in a single fibroblast. Cell Motil Cytoskeleton. 2004; 59(4):242–248. [PubMed: 15493061]
34. Mizutani T, Kawabata K, Koyama Y, Takahashi M, Haga H. Regulation of cellular contractile force in response to mechanical stretch by diphosphorylation of myosin regulatory light chain via RhoA signaling cascade. Cell Motil Cytoskeleton. 2009; 66(7):389–397. [PubMed: 19444895]

35. Haga H, Sasaki S, Kawabata K, Ito E, Ushiki T, Sambongi T. Elasticity mapping of living fibroblasts by AFM and immunofluorescence observation of the cytoskeleton. Ultramicroscopy. 2000; 82(1–4):253–258. [PubMed: 10741677]
36. Ito M, Yamagata T. Purification and characterization of glycosphingolipid-specific endoglycosidases (endoglycoceramidases) from a mutant strain of Rhodococcus sp. Evidence for three molecular species of endoglycoceramidase with different specificities. J Biol Chem. 1989; 264(16):9510–9519. [PubMed: 2722847]
37. Fujitani N, Takegawa Y, Ishibashi Y, Araki K, Furukawa J, Mitsutake S, et al. Qualitative and Quantitative Cellular Glycomics of Glycosphingolipids Based on Rhodococcal Endoglycosylceramidase-assisted Glycan Cleavage, Glycoblotting-assisted Sample Preparation, and Matrix-assisted Laser Desorption Ionization Tandem Time-of-flight Mass Spectrometry Analysis. J Biol Chem. 2011; 286(48):41669–41679. [PubMed: 21965662]
38. Sabatini M, Thomas M, Deschamps C, Lesur C, Rolland G, de Nanteuil G, et al. Effects of ceramide on aggrecanase activity in rabbit articular cartilage. Biochem Biophys Res Commun. 2001; 283(5):1105–1110. [PubMed: 11355886]
39. Sabatini M, Rolland G, Leonce S, Thomas M, Lesur C, Perez V, et al. Effects of ceramide on apoptosis, proteoglycan degradation, and matrix metalloproteinase expression in rabbit articular cartilage. Biochem Biophys Res Commun. 2000; 267(1):438–444. [PubMed: 10623638]
40. Chambers MG, Cox L, Chong L, Suri N, Cover P, Bayliss MT, et al. Matrix metalloproteinases and aggrecanases cleave aggrecan in different zones of normal cartilage but colocalize in the development of osteoarthritic lesions in STR/ort mice. Arthritis Rheum. 2001; 44(6):1455–1465. [PubMed: 11407708]
41. Memon RA, Holleran WM, Uchida Y, Moser AH, Ichikawa S, Hirabayashi Y, et al. Regulation of glycosphingolipid metabolism in liver during the acute phase response. J Biol Chem. 1999; 274(28):19707–19713. [PubMed: 10391911]
42. Choo YK, Ichikawa S, Hirabayashi Y. Developmental patterns of ceramide glucosyltransferase (GlcT-1) expression in the mouse: in situ hybridization using DIG-labeled RNA probes. Mol Cells. 2001; 11(3):346–351. [PubMed: 11459225]
43. Hakomori S, Igarashi Y. Functional role of glycosphingolipids in cell recognition and signaling. J Biochem. 1995; 118(6):1091–1103. [PubMed: 8720120]
44. van Echten G, Sandhoff K. Ganglioside metabolism. Enzymology, Topology, and regulation. J Biol Chem. 1993; 268(8):5341–5344. [PubMed: 8449895]

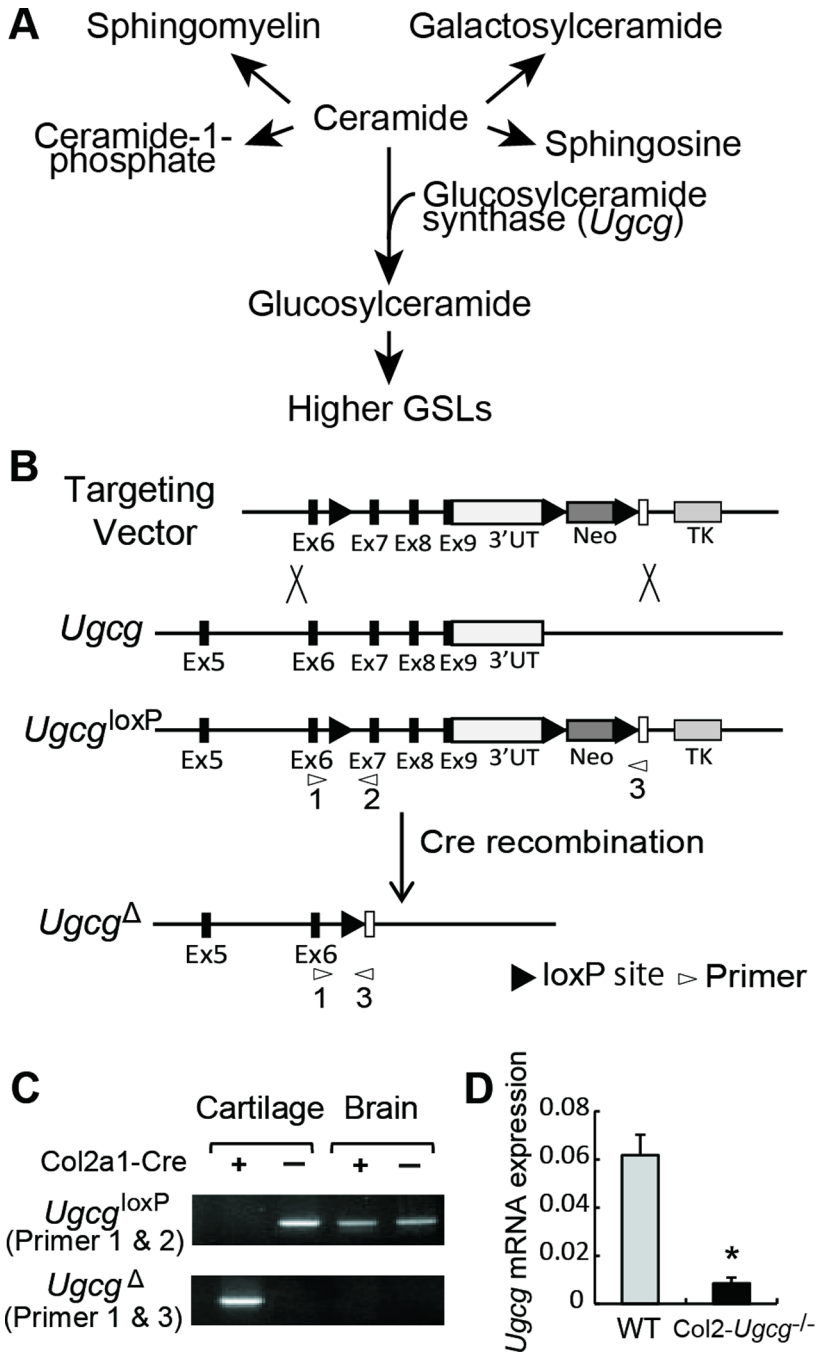


**Figure 1.**

*Ugcg* gene targeting. **A**, Biosynthetic pathways for GSLs. **B**, Schema of the *Ugcg* targeting strategy and cre-mediated recombination of the $Ugcg^{loxP}$ allele. UT, untranslated region; Neo, neomycin cassette; TK, thymidine kinase; Probe, location of probe used to select clones. **C**, Identification of cre-mediated recombination of the $Ugcg^{loxP}$ allele in cartilage. Genomic DNA from cartilage and brain was subjected to PCR using primers 1 and 2 to detect the $Ugcg^{loxP}$ allele and primers 1 and 3 to detect the $Ugcg^{\Delta}$ allele. Locations of PCR primers are shown in **B. D**, Expression of *Ugcg* mRNA in articular cartilage from wild-type

(WT) and Col2-*Ugcg*$^{-/-}$ mice determined by real time RT-PCR (n = 3 per group). Data shown are mean ± SEM. * = $P < 0.05$.

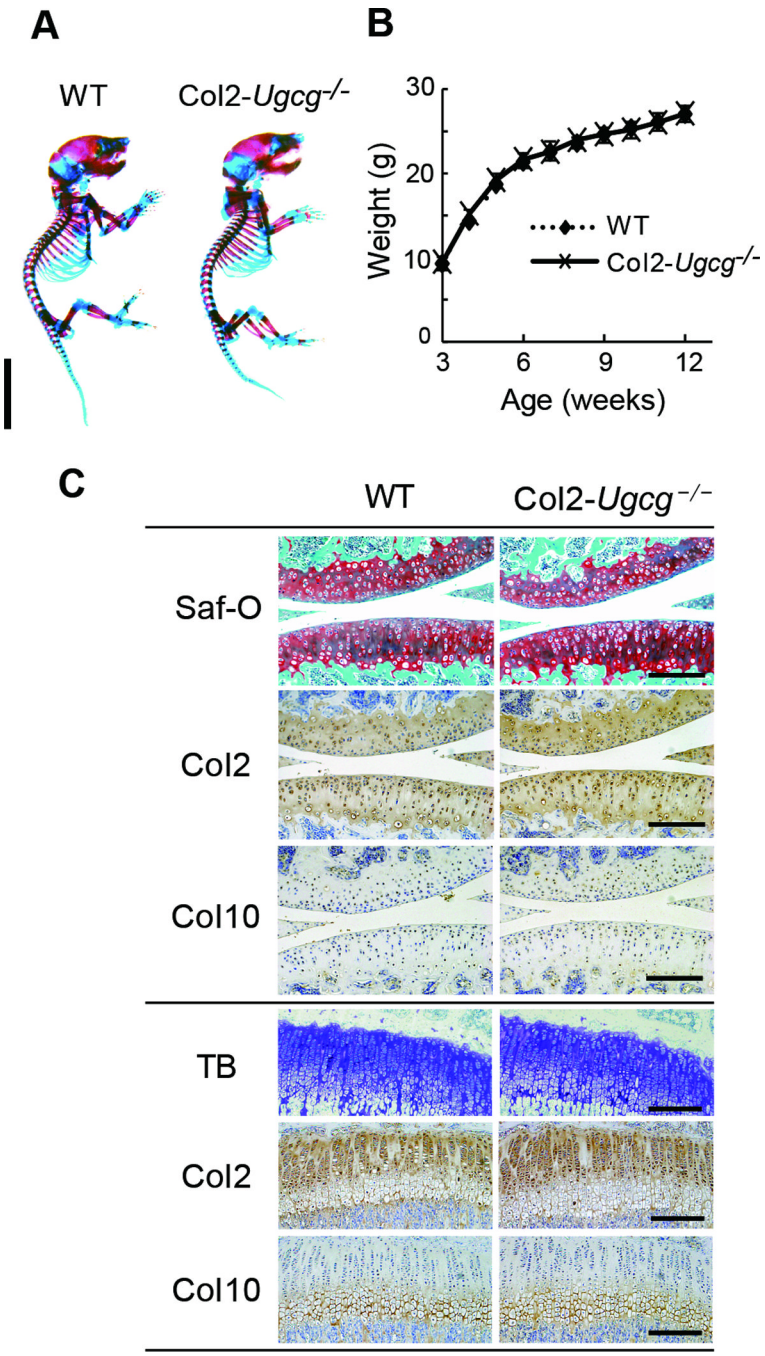


**Figure 2.**

The phenotype of young mice. **A**, Double staining with alcian blue and alizarin red of the whole skeleton in newborn mice. Scale bar = 1 cm. **B**, Growth curves determined by the body weight of male wild-type (WT) and Col2-*Ugcg*$^{-/-}$ littermates. Weight did not differ significantly between genotypes (n = 10 per group). Data shown are mean ± SEM. Females of both genotypes showed similar skeletal development and growth (data not shown). **C**, Histological findings of the knee joints in 4-week-old mice. Safranin O (Saf-O) staining, toluidine blue (TB) staining, and immunostaining of type II collagen (Col2) and type X

collagen (Col10) were performed in each genotype (upper: articular cartilage, lower: growth plate of tibia). Scale bars = 100 μm.

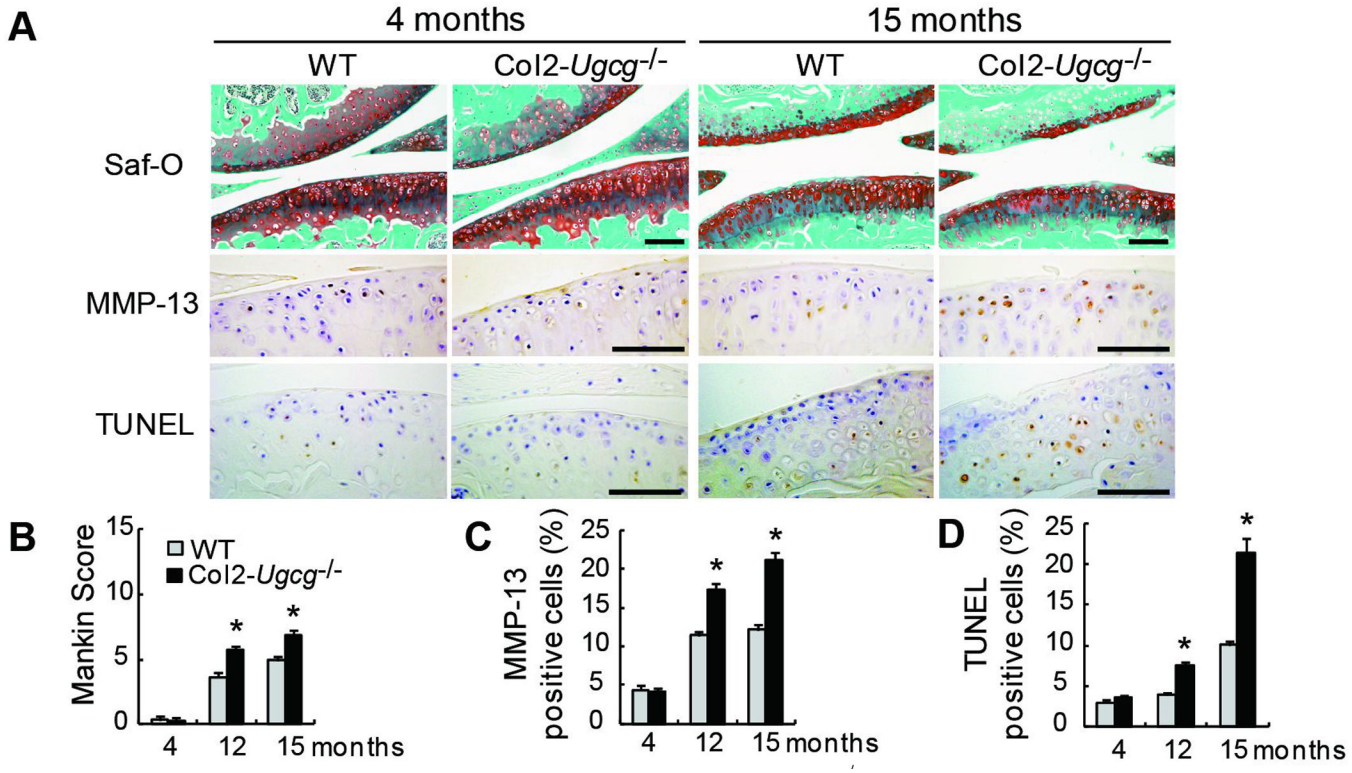


**Figure 3.**

Histological findings of age-associated OA in wild-type (WT) and Col2-*Ugcg*$^{-/-}$ littermates. **A**, Histological findings of age-associated OA. Safranin-O (Saf-O) staining (top; knee joint), immunostaining of MMP-13 (middle; proximal tibia), and TUNEL staining (bottom; proximal tibia). Scale bars = 100 μm. **B**, Mankin score of WT and Col2-*Ugcg*$^{-/-}$ littermates (n = 10 per group). **C**, The percentage of MMP-13 positive staining cells in WT and Col2-*Ugcg*$^{-/-}$ littermates (n = 10 per group). **D**, The percentage of TUNEL-positive staining cells in WT and Col2-*Ugcg*$^{-/-}$ littermates (n = 10 per group). Data shown are mean ± SEM. * = $P < 0.01$.

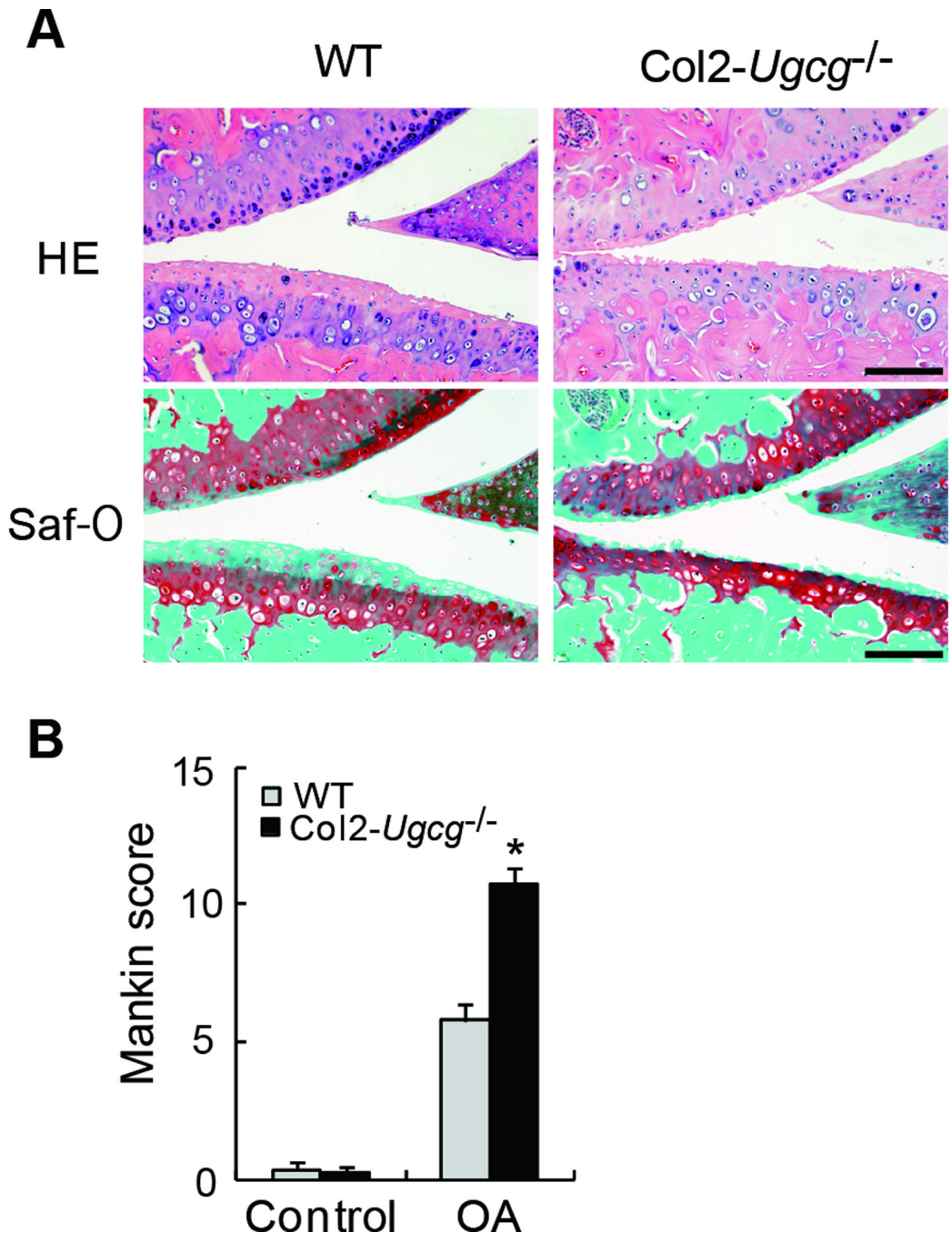


**Figure 4.**

Histological findings of instability-induced OA in wild-type (WT) and Col2-*Ugcg*$^{-/-}$ littermates 8 weeks after surgery. **A,** HE staining (top) and safranin-O (Saf-O) staining (bottom). Scale bars = 100 μm. **B**, Mankin score of WT and Col2-*Ugcg*$^{-/-}$ littermates (n = 8 per group). Data shown are mean ± SEM. * = $P < 0.01$.

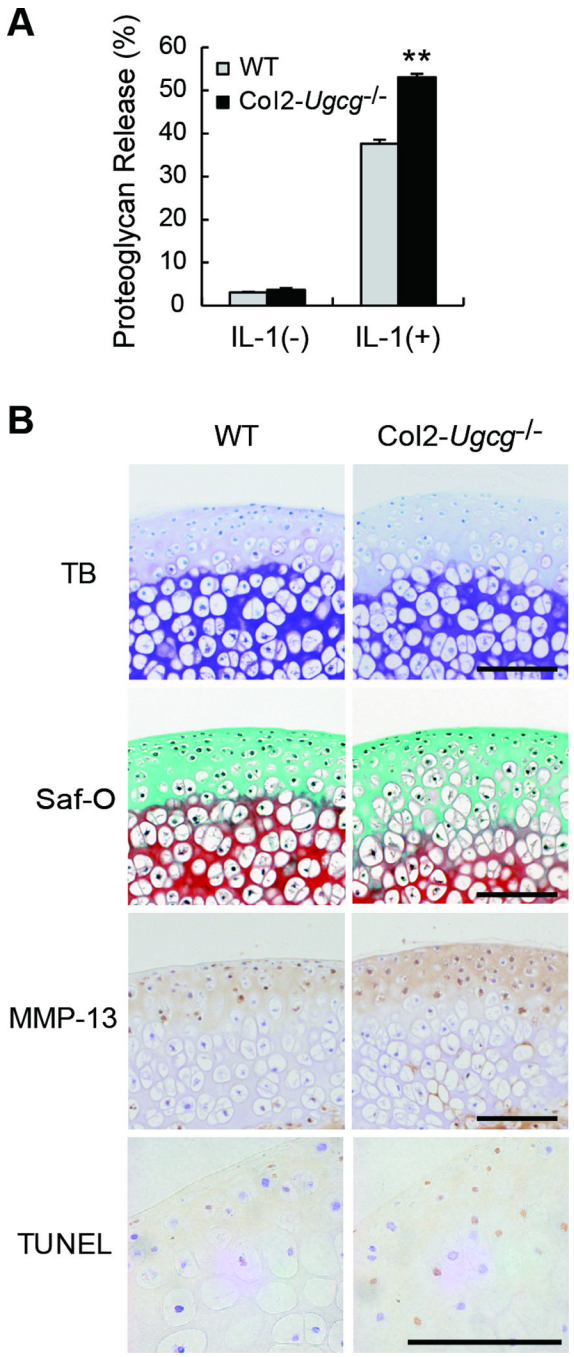


**Figure 5.**

Cartilage degradation induced by IL-1α stimulation. **A**, Proteoglycan release in cultured cartilage explants from wild-type (WT) and Col2-*Ugcg*$^{-/-}$ littermates (n = 5 per group). Data shown are mean ± SEM. * = $P < 0.01$, ** = $P < 0.05$. **B**, Histological findings of cartilage explants cultured with IL-1α from WT and Col2-*Ugcg*$^{-/-}$ littermates (from top to bottom, TB, toluidine blue; Saf-O, safranin O; MMP-13 immunostaining, and TUNEL staining). Scale bars = 100 μm.

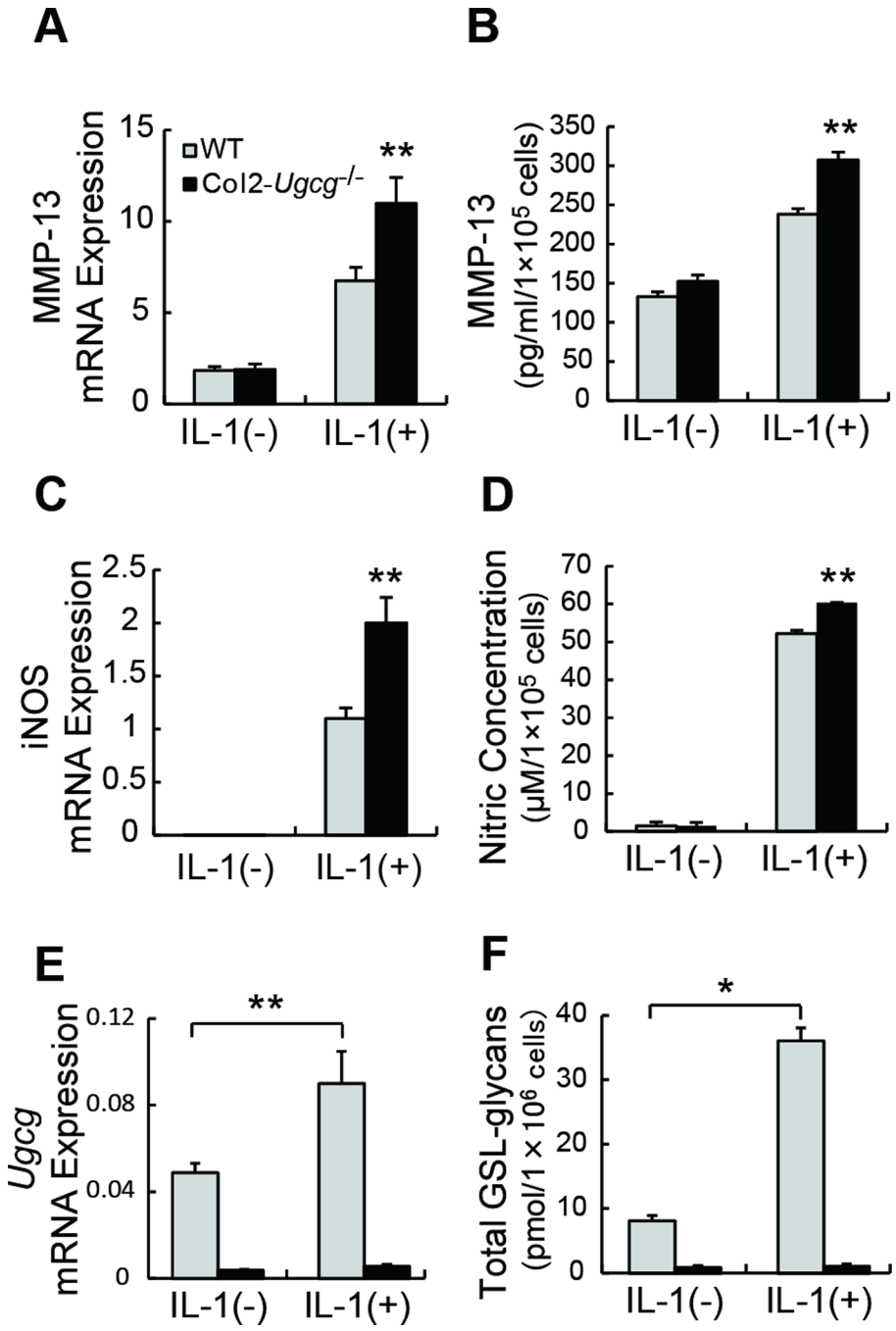


**Figure 6.**

Chondrocyte reaction induced by IL-1α stimulation. **A**, Expression of MMP-13 mRNA in cultured chondrocytes determined by real-time RT-PCR (n = 5 per group). **B**, Quantification of MMP-13 release in chondrocyte culture supernatant determined by ELISA (n = 5 per group). **C**, Expression of inducible nitric oxide synthase (iNOS) mRNA in cultured chondrocytes determined by real-time RT-PCR (n = 5 per group). **D**, Quantification of nitric oxide (NO) release in chondrocyte culture supernatant (n = 5 per group). **E**, Expression of *Ugcg* mRNA in cultured chondrocytes determined by real-time RT-PCR (n = 5 per group).

**F**, Quantification of total GSL-glycans in cultured chondrocyte pellets. (n = 3 per group). Data shown are mean ± SEM. * = $P < 0.01$, ** = $P < 0.05$.